

Some Insights on the Use of Polyols-Based Metal Alkoxides Powders as Precursors for Tailored Metal-Oxides Particles

D. Larcher,* G. Sudant, R. Patrice, and J.-M. Tarascon

Laboratoire de Réactivité et Chimie des Solides and CNRS UMR 6007, 33, rue Saint Leu, 80039 Amiens Cedex, France

Received February 21, 2003. Revised Manuscript Received May 28, 2003

In this paper, we describe the synthesis of tailor-made cobalt and manganese oxides by a two-step preparation method. The first step consists of precipitating metal alkoxide powders from aliphatic polyalcohol solutions of salts. Their particle size, composition, and morphology can be independently tuned by controlling the precipitation conditions (type of alcohol and concentration). The second step involves thermal decomposition under air, leading to crystalline metal oxides, whose specific surface area and crystallite size can be adjusted by a careful selection of the alcohol used and the annealing temperature. More specifically, we found that the crystallite size of these oxides is determined by the amount of heat released during the combustion of the organic component. Since the size and morphology of the precursors are strictly maintained during the pyrolysis treatment, we can therefore achieve an accurate control of the different aspects of the texture of metal oxide powders. Preliminary results show that this approach can be successfully extended to bimetallic phases.

Introduction

The control of the morphology, size, and texture of active powders is a major issue in fields such as sensors, solid-state electrochemistry, electrochromism, and catalysis where phenomena are highly dependent on surface/interface reactions. In this context, any synthetic approach enabling the control of the powders characteristics is therefore of great interest. Although numerous synthetic methods are available, none of them are presently able to allow independent control of all these aspects.

Metal alkoxides $M(OR)_n$ are well-known and widely studied compounds but most of the related works have focused on the preparation, stability, and chemistry of monodentate alkoxides, such as ethoxides and isopropoxides. Since the first systematic study in the early 1950s, much of the literature has focused on these functionalized compounds, and their preparation as well as their reactivity are now well-documented.^{1–3} However, many other organic/inorganic hybrids have been prepared as crystalline powders by reacting a metallic salt in appropriate polyalcohols instead of monoalcohols. During the past 3 decades, this was punctually investigated for various metals (Co, Zn, Fe, Mn, Ti, Bi, Ni, Pb, Mo, etc.) and polyols (ethylene-glycol and glycerol)^{4–15}

and a few mixed materials such as (Fe,Mn)-glycerol, (Ba,Ti)-ethylene glycol, (Al,Fe)-glycerol, and (Si, alkaline earth)-ethylene glycol, for example.^{7,16–21}

It has been reported that the thermal decomposition of these materials generally results in the formation of metal oxides at temperatures close to that of the combustion of the organic component. Surprisingly, this synthesis procedure is rarely described in the literature, and only a few reports are devoted to some specific aspects.^{7,14–24}

In this paper, we show that the morphology, size, and texture of metal oxide powders can be independently tuned by adjusting (1) the precipitation conditions of the alkoxide precursors and (2) the conditions of the de-

- (1) Mehrotra, R. C. *J. Non-Cryst. Solids* **1988**, *100*, 1.
- (2) Hubert-Pfalzgraf, L. G. *Coord. Chem. Rev.* **1998**, *178–180*, 967.
- (3) Bradley, review alkoxides.
- (4) Radoslovich, E. W.; Raupach, M.; Slade, P. G.; Taylor, R. M. *Aust. J. Chem.* **1970**, *23*, 1963.
- (5) Fuls, P. F.; Rodrique, L.; Fripiat, J. J. *Clays Clay Miner.* **1970**, *18*, 53.
- (6) Slade, P. G.; Radoslovich, E. W.; Raupach, M. *Acta Crystallogr.* **1971**, *B27*, 2432.
- (7) de Simoni, C. Ms.Sc, Université catholique de Louvain.
- (8) Schröder, F. A.; Scherle, J. *Acta Crystallogr.* **1975**, *B31*, 531.

- (9) Wang, D. Yu, R.; Kumada, N.; Kinomura, N. *Chem. Mater.* **1999**, *11*, 2008.
- (10) Saadoun, L. et al. *Appl. Catal., B* **1999**, *21*, 269.
- (11) Tekaiia-Elhsissen, K.; Delahaye-Vidal, A.; Nowogrocki, G.; Figlarz, M. C. *R. Acad. Sci. Paris* **1989**, *309(II)*, 349.
- (12) Fedorov, F.; Sokolova, N. A. *J. Appl. Chem.* **1971**, *44*, 2265.
- (13) Cloutt, B. A.; Sagatys, D. S.; Smith, G.; Bott, R. C. *Aust. J. Chem.* **1997**, *50*, 947.
- (14) Larcher, D.; Sudant, G.; Leriche, J. B.; Chabre, Y.; Tarascon, J. M. *J. Electrochem. Soc.* **2002**, *149(3)*, A234–A241.
- (15) Larcher, D.; Gérard, B.; Tarascon, J. M. *J. Solid State Electrochem.* **1998**, *2(3)*, 137–145.
- (16) Day, V. W.; Eberspacher, T. A.; Frey, M. H.; Klemperer, W. G.; Liang, S.; Payne, D. A. *Chem. Mater.* **1996**, *8(2)*, 331.
- (17) Mendelovici, E.; Villalba, R.; Sagarzazu, A. *J. Mater. Sci. Lett.* **1990**, *9*, 28.
- (18) Mendelovici, E.; Sagarzazu, A.; Villalba, R. *Thermochim. Acta* **1986**, *107*, 75.
- (19) Laine, R. M. et al. *Nature* **1991**, *353*, 642.
- (20) Blohowiak, K. Y. et al. *Chem. Mater.* **1994**, *6*, 2177.
- (21) Kansal, P.; Laine, R. M. *J. Am. Ceram. Soc.* **1995**, *78(3)*, 529.
- (22) Wiedemann, H. G.; Nerbel, J.; Reller, A. *Thermochim. Acta* **1998**, *318*, 71.
- (23) Thoms, H.; Eppe, M.; Reller, A. *Solid State Ionics* **1997**, *101–103*, 79.
- (24) Thoms, H.; Eppe, M.; Reller, A. *Thermochim. Acta* **1997**, *3375*, 195.

Table 1. Nature and Composition of the Phases Obtained by Reaction of Co (160 °C) and Mn (Boiling Point) Hydrated Acetate Solutions in Different Polyalcohols^a

		Mn acetate + LiOH			Co acetate		
		name and proposed formula	weight loss	wt % exp. (calc.)	name and proposed formula	weight loss	wt % exp. (calc.)
2-carbon chain	ethylene glycol (EG)	Mn-EG Mn(EG ²⁻) _{1.01} (OH ⁻) _ε	31.5%	Mn: 48.1 (47.6) O: 28.0 (28.0) H: 3.3 (3.5) C: 20.6 (21.0)	Co-EG Co(EG ²⁻) _{0.46} (EG ²⁻) _{0.77}	39.6%	Co: 43.2 (44.3) O: 30.6 (29.6) H: 4.2 (3.9) C: 22.0 (22.2)
	1,2-propanediol (Pro12)	Mn-Pro12 Mn(Pro12 ²⁻) _{0.97} (OH ⁻) _ε	37.6%	Mn: 43.5 (43.4) O: 25.1 (24.5) H: 4.4 (4.6) C: 27.0 (27.5)	Co-Pro12 Co(Pro12 ²⁻) _{0.47} (Pro12 ²⁻) _{0.76}	47.4%	Co: 40.2 (39.3) O: 25.2 (26.2) H: 6.0 (5.0) C: 28.6 (29.5)
3-carbon chains	1,3-propanediol (Pro13)	Mn-Pro13 Mn(Pro13 ²⁻) _{0.97} (OH ⁻) _ε	37.5%	Mn: 44.0 (43.4) O: 24.1 (24.5) H: 4.8 (4.6) C: 27.1 (27.5)	Co-Pro13 Co(Pro13 ²⁻) _{0.18} (Pro13 ²⁻) _{0.91}	43.5%	Co: 41.9 (42.2) O: 25.5 (25.0) H: 5.0 (4.7) C: 27.6 (28.1)
	glycerol (Gly)	Mn-Gly Mn(Gly ²⁻) _{0.65} (Gly ³⁻) _{0.23}	39.6%	Mn: 41.5 (41.0) O: 31.0 (31.6) H: 3.7 (3.8) C: 23.8 (23.6)	Co-Gly Co(Gly ²⁻) _{1.06}	46.9%	Co: 38.5 (38.2) O: 33.5 (32.9) H: 4.0 (4.2) C: 25.0 (24.7)
	1,2-butanediol (But12)	Mn-But12 Mn(But12 ²⁻) _{0.97} (OH ⁻) _ε	43.9%	Mn: 39.0 (39.2) O: 21.5 (22.1) H: 5.7 (5.5) C: 33.8 (33.2)	Co-But12 Co(But12 ²⁻) _{0.36} (OH ⁻) _{1.64}	32.7%	Co: 50.5 (49.7) O: 31.5 (31.9) H: 4.0 (3.8) C: 14.0 (14.6)
4-carbon chains	1,3-butanediol (But13)	/	/	/	Co-But13 Co(But13 ²⁻) _{0.2} (OH ⁻) _{1.8}	26.2%	Co: 54.1 (54.9) O: 33.1 (32.8) H: 3.4 (3.4) C: 9.4 (8.9)
	1,4-butanediol (But14)	/	/	/	/		
	2,3-butanediol (But23)	Mn-But23 Mn(But23 ²⁻) _{0.97} (OH ⁻) _ε	43.5%	Mn: 38.7 (39.2) O: 22.2 (22.1) H: 5.5 (5.5) C: 33.6 (33.2)	Co-But23 Co(But23 ²⁻) _{0.36} (OH ⁻) _{1.64}	32.8%	Co: 48.3 (49.6) O: 31.0 (31.8) H: 4.0 (4.1) C: 16.7 (14.5)

^a Weight losses are those measured from TGA analysis, from 150 to 800 °C under air. Products recovered at 800 °C are identified as Mn₂O₃ and Co₃O₄.

composition treatment. With the aid of this method and the accurate control it conveys, we have already identified a close relation between the specific surface area of Co₃O₄ powders and their electrochemical reactivity toward metallic lithium¹⁴ and have achieved the preparation of single and mixed oxides with unusual lamellar morphology.¹⁵

Given the numerous phases that can be prepared by reacting metallic salts in alcohols and the numerous synthesis/decomposition combinations that can be tested, we will limit our discussion to cobalt- and manganese-alkoxides.

Materials and Methods

Characterization Techniques. Phase identification was carried out by means of X-ray diffraction (XRD, Philips PW 1729) using Cu Kα radiation ($\lambda = 1.5418$ Å) and a diffracted beam monochromator.

Specific surface area and porosity were determined using the BET and BJH multipoints methods from results of N₂ physisorption at 77 K with a Micromeritics 2375 Gemini analyzer.^{25,26} Samples were preheated for 1 h at 150 °C under argon flow.

Thermogravimetric analysis (TGA) and differential scanning calorimetry (DSC) data were collected at a heating rate of 5 °C/min under static air using a Mettler apparatus and an open

alumina holder. For TGA, all the data were corrected for the variations of the buoyancy of the sample container itself. All samples were preheated to 150 °C for 1 h to remove adsorbed water/alcohol.

Scanning electron microscopy (SEM) images were obtained with a FEG XL-30 microscope equipped with a Link ISIS EDS (energy-dispersive spectroscopy) probe, which allows determination of the relative metallic contents for bimetallic phases.

Infrared (IR) spectra were obtained at room temperature with a Nicolet 510 FT-IR spectrophotometer. For that, a few milligrams of powder was mixed with 200 mg of KBr dried at 125 °C and pelletized at 8 t/cm².

Materials Synthesis. Co and Mn acetates and eight polyalcohols (polyols) with 2-, 3-, and 4-carbon backbones (ethylene glycol; glycerol; 1,2- and 1,3-propanediols; 1,2-, 1,3-, 1,4-, and 2,3-butanediols) have been used in this study.

Preparation of metal alkoxides involved dissolving hydrated M(II) acetate at ambient temperature in the liquid polyol. Typically, 0.2–4 g of acetate was used for 200 mL of alcohol. To ease the in situ formation of alcoholate ions, and therefore the precipitation of manganese-based alkoxides, 0.1 M of anhydrous LiOH was simultaneously dissolved in the reacting medium. The resulting solution was then heated to a selected temperature at a rate of 5 °C/min under reflux and constant stirring. Care has to be exercised in the choice of the reaction temperatures. Indeed, the temperature has to be high enough to ensure the alkoxide precipitation, but in the case of cobalt, it also has to be limited to avoid the complete reduction of Co²⁺ by the alcohol into metallic cobalt. The optimized heating temperatures were fixed at 160 °C for Co and at the boiling point for Mn, whatever the alcohol tested. As soon as a precipitate was visible, frequent and regular withdrawals of the hot suspension were performed, from which the precipitate

(25) Brunauer, S.; Emmett, P. H.; Teller, E. *J. Am. Chem. Soc.* **1938**, *60*, 309.

(26) Barrett, E. P.; Joyner, L. G.; Hallender, P. C. *J. Am. Chem. Soc.* **1951**, *73*, 373.

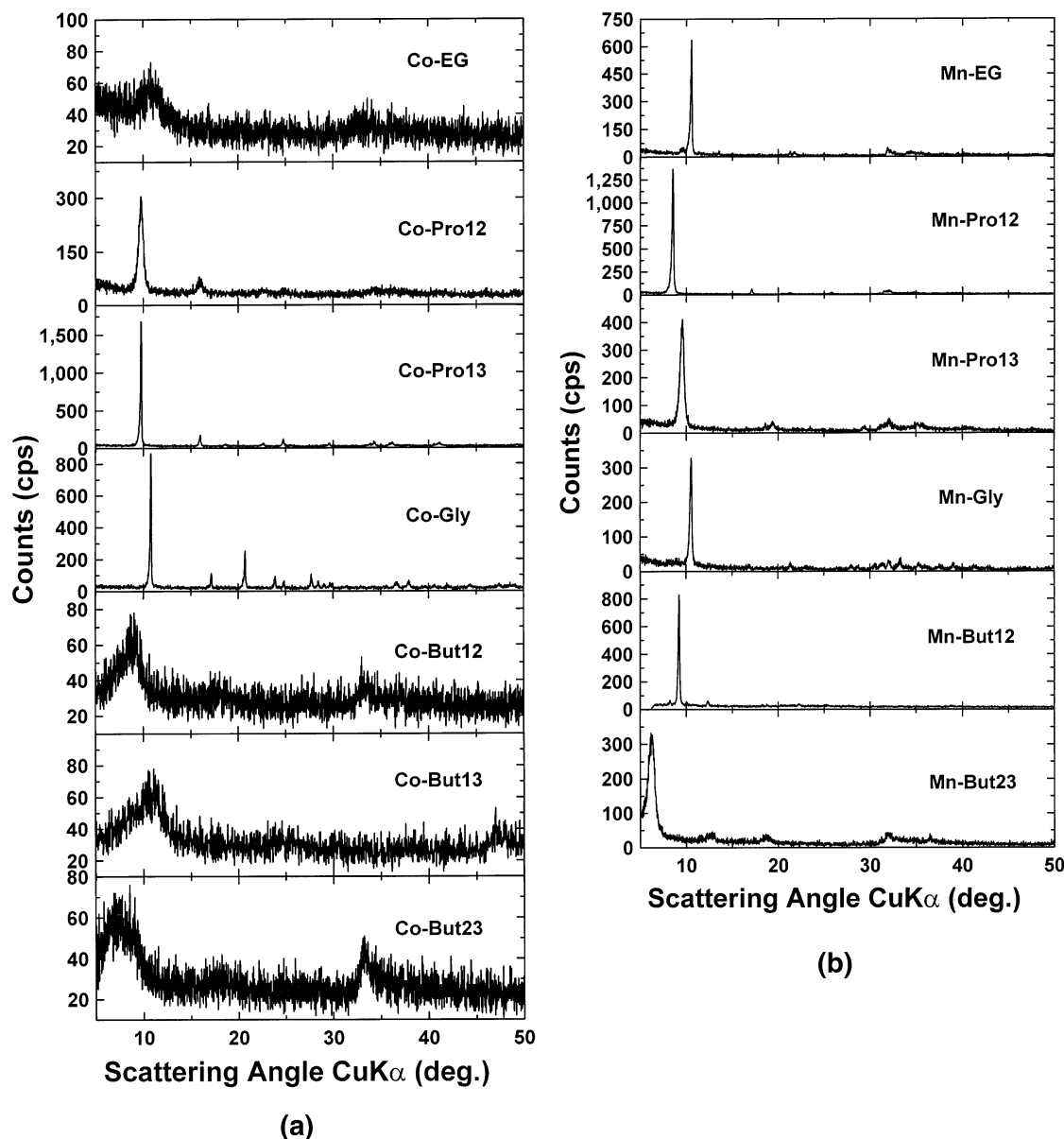


Figure 1. X-ray diffraction patterns of (a) Co and (b) Mn alkoxides prepared by reaction of metal acetates in different polyalcohols.

was extracted by filtration or centrifugation depending on the viscosity of the liquid. Then, recovered solids were washed with pure polyol and ethanol and dried for a few hours at 50 °C. The structure of these powders was immediately checked by X-ray diffraction and their organic contents by infrared spectroscopy. When the formation of an alkoxide was detected without any trace of byproducts (e.g., acetate, metal, oxide, etc.), the main suspension was cooled to ambient temperature and the batch powder recovered as for the withdrawn samples. Generally, the alkoxide precipitation happened after a few hours of reaction. Due to their slight long-term instability toward moisture, these alkoxide powders were stored in an argon-filled glovebox.

Thermal decomposition of the alkoxides was achieved under airflow in a muffle furnace at a heating rate of 5 °C/min up to different dwell temperatures maintained for 1 h.

Results and Discussions

For sake of clarity, a simple nomenclature was adopted to easily identify our samples. For instance, the Mn alkoxide prepared in ethylene glycol will be called Mn-EG, and that prepared from cobalt acetate and 2,3-

butanediol will be referred to as Co-But23 (see Table 1).

Figure 1a,b presents the X-ray diffraction patterns of Co and Mn alkoxides synthesized in this research work. All these patterns mainly exhibit a strong low-angle reflection related to interlayer spacing in lamellar structures.^{4–6,11,15} Basically, these structures are described as stacked metal–oxygen sheets separated by bonded alcoholate anions. In contrast to what one could expect, no reliable trend appears between the interlayer distance and the size of the alcohol molecule. In addition, the lack of structural information about these materials and the similarity between their XRD patterns do not allow their identification from XRD. To our advantage, this was partially compensated by the presence of organic components in the structures and therefore the use of infrared spectroscopy as an accurate identification tool. This is illustrated in Figure 2 for Mn-based materials. The strong absorption bands lying in the 2500–3000-cm^{–1} domain are characteristic of the

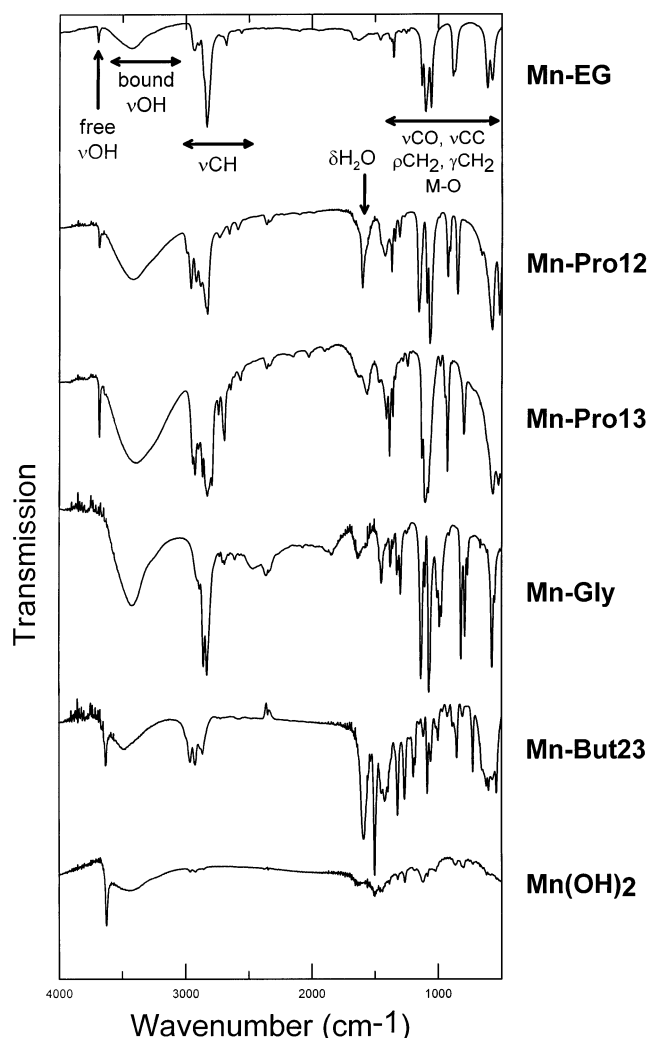


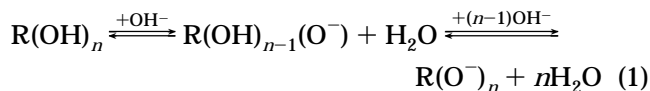
Figure 2. Infrared spectra for Mn-based alkoxide powders. Characteristic C–H stretching vibrations are observed in the 2500–3000-cm⁻¹ region. The spectrum of Mn(OH)₂ is also displayed for sake of comparison.

C–H stretching mode. The wide hump centered at 3400 cm⁻¹, the sharp band at ca. 3600 cm⁻¹, and that at 1620 cm⁻¹ are attributed to hydrogen-bound hydroxyl groups, structurally isolated hydroxyls (i.e., Mn(OH)₂ hydroxide-type), and δH₂O bending signal, respectively. With the exception of this δH₂O vibration, all the bands located below 2000 cm⁻¹ are due to metal–O, C–C, C–O, and CH₂ bonds. Upon heating at 150 °C or vacuum treatment, this characteristic δH₂O-bending signal disappears, indicating the departure of surface water. Even when this band totally disappeared, the signal at 3400 cm⁻¹ remained, clueing for structural loosely bonded OH groups. The presence of structurally free OH functions and organic groups is also confirmed by the fact that their characteristic signals are not affected by this heating treatment. Note that the absence of absorption around 1700 cm⁻¹ eliminates the possibility of carboxyl groups, and therefore the presence of remaining acetate groups in the materials.

The elemental composition (metal, C, O, and H) of the Mn- and Co-based powders was determined by chemical analysis, whereas thermogravimetric analysis was used to calculate the molecular weight of the alkoxides from the overall weight loss and the composition of the final

pyrolyzed products. Since all the reactions were conducted with M²⁺-containing reagents dissolved in reducing media, higher oxidation states (e.g., Mn³⁺ and Co³⁺) are highly unlikely in the precipitates. All these data lead to the compositions listed in Table 1. Our results on glycerol-based phases (XRD, infrared spectroscopy, and composition) are in perfect agreement with previously reported data.^{4,6}

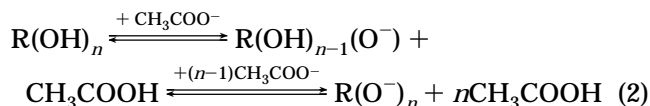
Basically, the precipitation of the alkoxides is highly dependent on the nature of the anionic composition of the medium. These anionic species can be hydroxide, acetate, or totally/partially deprotonated alcohols resulting from acid–base equilibrium reactions. In the presence of strong alkali, the main reaction is



$n = 2$ for diols, $n = 3$ for triol (glycerol)

This is consistent with the results presented in Table 1, showing that the Mn-based alkoxides contain totally or highly deprotonated alcohols. This highly basic media also accounts for the presence of small amounts of structural hydroxyl groups (Figure 2).

In the case of cobalt, no strong base being added, the formation of alcoholate ions and hydroxyls groups are therefore not so trivial, and only the intrinsically weak basicity of the acetate counterion can affect this issue. Acetate ions can react with alcohol or with water molecules, resulting from the dissolution of the hydrated acetate salts, as follows:



This agrees well with the presence of partially deprotonated polyols and a high amount of hydroxyl groups in Co-based samples. The remaining OH groups along the backbone of such partially deprotonated alcohols can also account for the broad infrared absorption band observed at 3400 cm⁻¹ on water-free heated samples.

Control of Composition, Size, and Morphology of the Alkoxides Precursors. As depicted in Figure 3, the majority of Co and Mn powders exhibit very well-defined morphologies (spheres, polyhedra, twinned, or isolated platelets) and only the Mn-Pro13 sample exhibits no defined particle shape, indicating a direct link between the composition (metal/polyol) of the powders and their morphology. Note also that the obtained powders are monodisperse. In addition, the particle morphology can be deliberately modified using alcohol mixtures. For example, one can change the polyhedral shape of Co-Pro13 to the spherical morphology of Co-Pro12 by adding a small amount (10%) of 1,2-propanediol to 1,3-propanediol (Figure 4). The infrared spectrum of this powder (Figure 4) reveals that it mainly contains 1,3-propanediol with a small amount of 1,2-propanediol. As will be seen later, the organic composition of these alkoxides is of major importance for the textural control of the oxides formed by their thermal

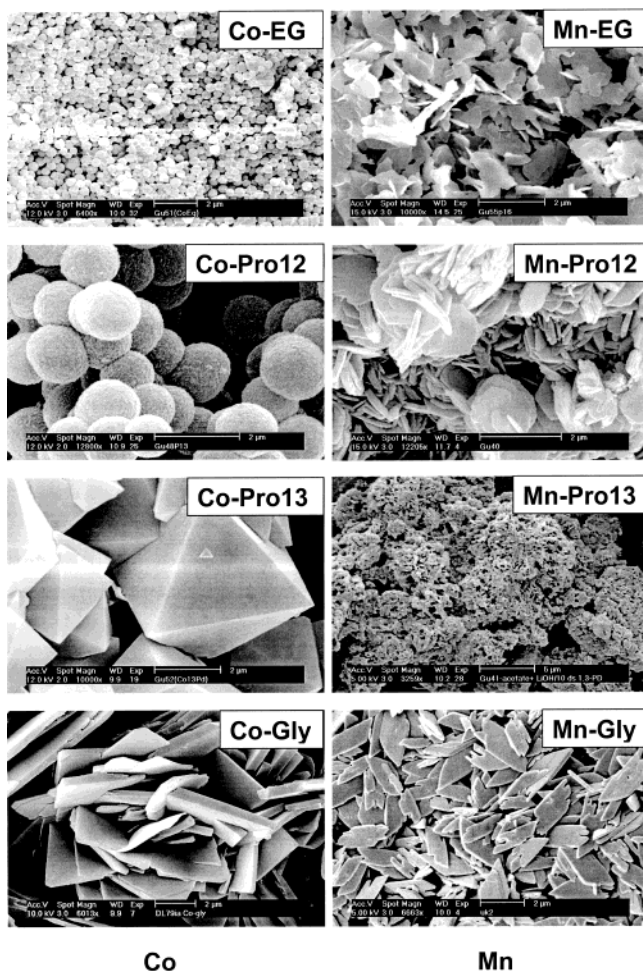


Figure 3. SEM pictures showing the morphology and size of some Co and Mn-alkoxides particles.

decomposition. Aside from the previously described strategy using polyol mixtures, we are presently explor-

ing the possibility of modifying this organic content, while keeping the morphology unchanged, through anionic exchange in various other polyalcohols. Despite very small differences in the relative pK_a values of the polyalcohols, these exchanges have already been reported in the case of (Si,alkaline-earth)-EG phases.^{19,21}

Provided the heating rate and plateau temperature are kept constant during the reaction of the polyol solutions, the size of the particles can also be easily controlled by adjusting the concentration of the dissolved salt. This is exemplified for Co-Pro12 spherical particles (Figure 5), whose size decreases from 1.4 to 0.3 μm when the amount of dissolved Co-acetate is decreased from 10 to 1 g/L. These powders exhibit a very narrow particle size distribution. The same effect has been observed for various alkoxides with different metal/polyol compositions.

The last point we would like to illustrate concerning the alkoxides preparation is the possibility of forming metal-mixed phases. This was, for instance, achieved for Mn/Co in 1,2-propanediol and glycerol. When the total amount of added acetate (10 g/L) is kept constant, different solutions were prepared by dissolving various (Mn-acetate/Co-acetate) ratios in these polyols and then treated as described in the Experimental Section. The recovered powders were analyzed by EDS for their metallic Mn/Co ratios, and the results were compared to the initial metallic contents (Figure 6). Whereas the initial Mn/Co ratio in solution coincides with that of the solid prepared in glycerol, it follows a curved relation for the powder prepared in 1,2-propanediol. This difference is not yet clearly understood but we could confirm that the precipitates are mixed-metal alkoxides (and not a mixture of pure Mn and Co phases) by following the XRD, infrared, and morphological evolutions while the Mn/Co contents were varied.

Having described our ability to prepare a complete panel of metal alkoxide powders with controlled size,

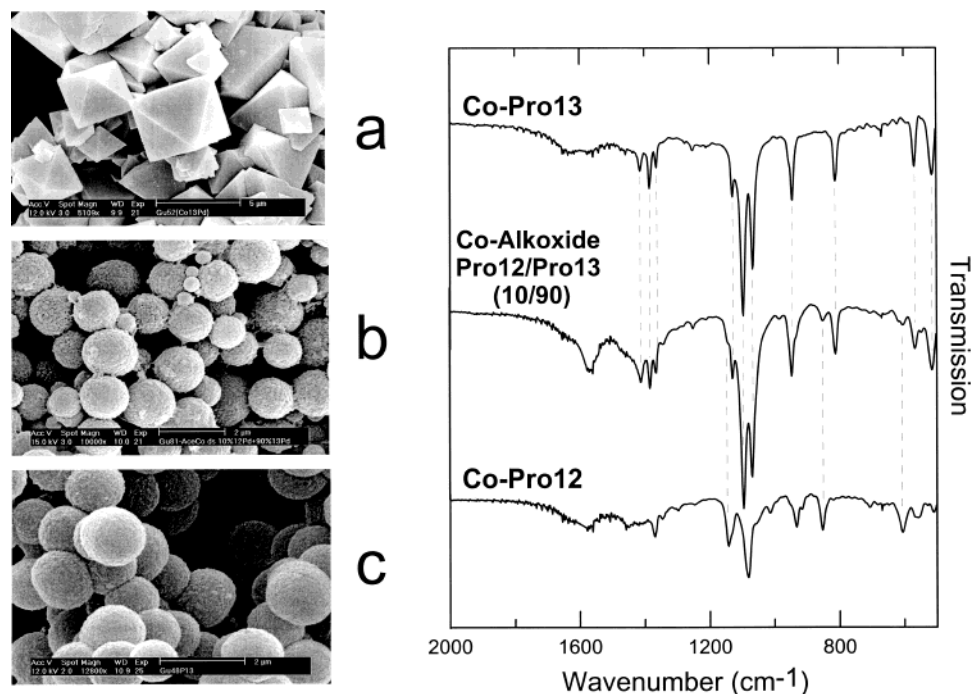


Figure 4. Evolution of the particles morphology and of the infrared spectra of Co-alkoxides with the liquid medium composition (1,2-propanediol, 1,3-propanediol, or 10/90 mixture of both).

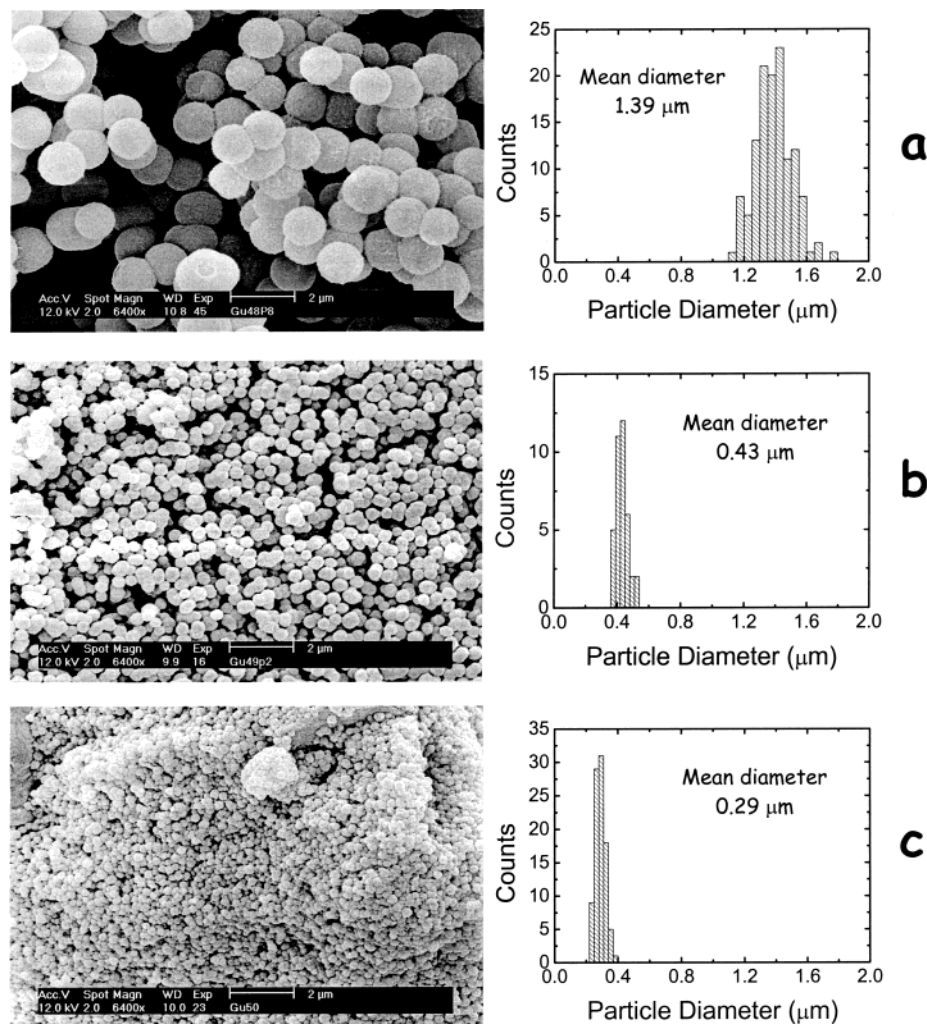


Figure 5. Particles size evolution as a function of Co-acetate concentration in the initial alcoholic solution (1,2-propanediol): (a) 10 g/L, (b) 2.5 g/L, and (c) 1 g/L.

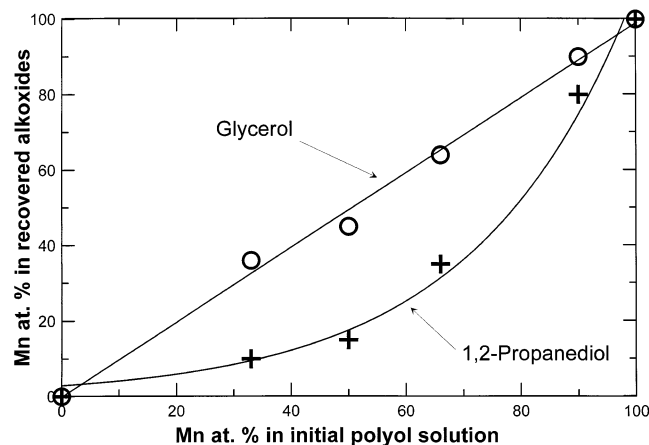


Figure 6. Relations between the Mn/Co atomic ratio in the solution (glycerol and 1,2-propanediol) and in the alkoxide powders recovered from heating of these solutions.

polyol/metal composition, and various selectable morphologies, we are now turning to their thermal decomposition.

Thermal Behavior of the Alkoxides Powders. Let us compare the TGA and DSC traces recorded from 150 to 800 °C under air (5 °C/min) for various Mn-based alkoxides (Figure 7). Each TGA curve is characterized by a very significant weight loss between 200 and 300

°C (Figure 7a) corresponding to a sharp DSC exothermic peak (Figure 7b). This weight loss can be ascribed to the decomposition of the organics, as confirmed by the infrared spectra recorded before and after the weight loss. Whatever the sample tested, the brown powders recovered after the combustion were identified as spinel Mn_3O_4 , and Mn_2O_3 is always obtained at 800 °C. This is illustrated in Figure 8 for Mn-Gly. This oxidation reaction can be visualized at around 500 °C as a small weight gain observed for Mn-EG, Mn-Pro12, and Mn-Gly. However, Mn-Pro13 behaves differently since the $\text{Mn}_3\text{O}_4 \rightarrow \text{Mn}_2\text{O}_3$ reaction proceeds through a progressive weight gain from 300 to about 500 °C followed by a weight loss at ca. 550 °C. This difference is clearly visible on the $\delta m/\delta T$ derivative curves (Figure 9). Such phenomenon has already been reported as nested in a difference in specific surface areas of the oxide. Low specific surface areas lead to direct oxidation, whereas high values ($>80 \text{ m}^2/\text{g}$) result in the formation of an unstable Mn_5O_8 oxidized intermediate.^{27,28} Therefore, the combustion of our alkoxides is likely to give rise to Mn_3O_4 materials with large differences in their specific surface areas, depending on the organic composition.

(27) Feitknecht, W. *Pure Appl. Chem.* **1964**, 9, 423.

(28) Gillot, B.; El Guendouzi, M.; Laarj, M. *Mater. Chem. Phys.* **2001**, 70, 54.

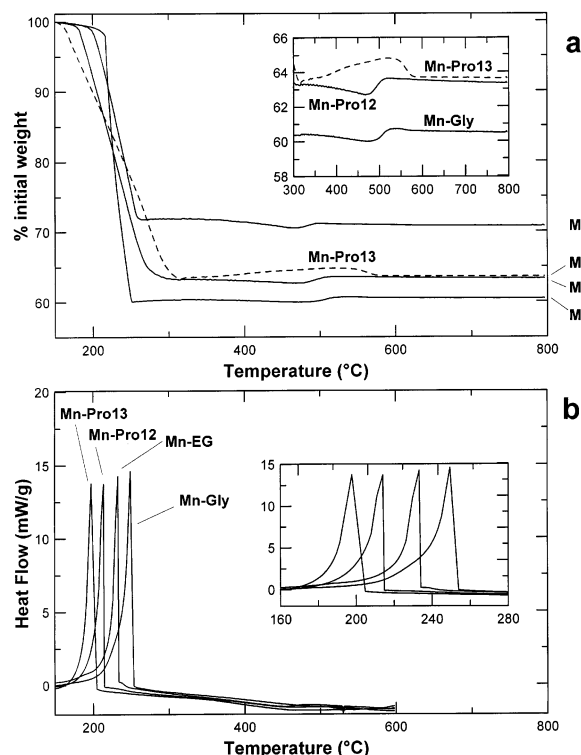


Figure 7. TGA and DSC traces for various Mn-based alkoxides (5 °C/min, air flow). Samples were preheated at 150 °C to remove adsorbed species.

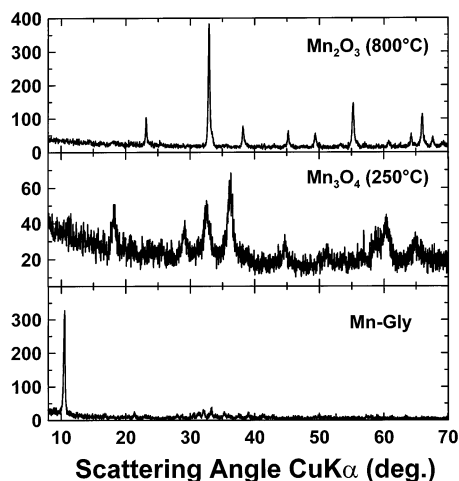


Figure 8. X-ray diffraction patterns of Mn-Gly precursor and of the oxides recovered after heating under air at 250 °C (Mn_3O_4) and at 800 °C (Mn_2O_3).

Samples were withdrawn in the course of the heating treatment and their specific surface areas measured (Figure 10). The oxides produced from Mn-Pro13 have the highest BET surface areas, reaching values far higher than 80 m^2/g during the heating. Since the maxima in BET values are observed at the temperature of the organics combustion, we can logically suppose the powder expansion to be directly linked to the volume of gaseous products this combustion releases. Would such a hypothesis be right, the higher the chain length (i.e., the higher the gas release), the higher the maximum in BET surface area. Although Mn-Pro12 and Mn-Pro13 have exactly the same chain length, they have totally different behavior, ruling out this hypothesis. A comparison between the data presented in Figures 7 and

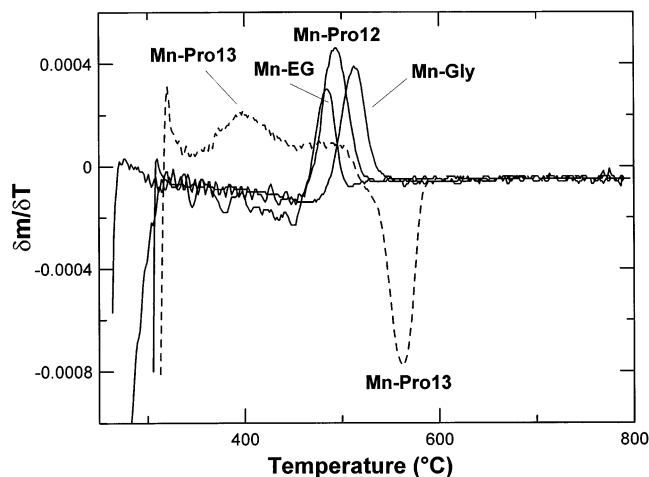


Figure 9. TGA derivative $\delta m/\delta T$ curves for different Mn-based alkoxides (5 °C/min, air flow).

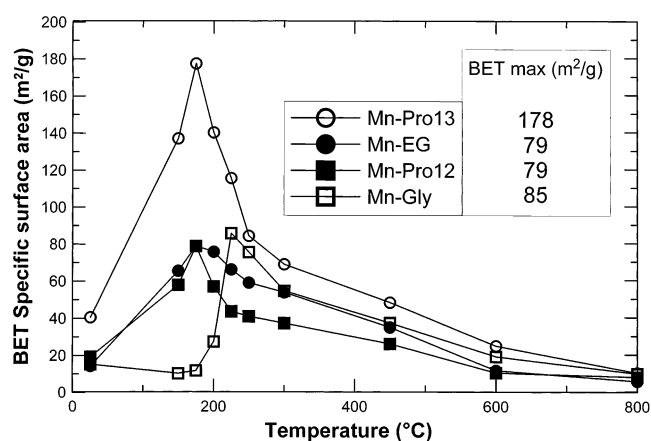


Figure 10. Evolution of the BET specific surface areas along the air-heating treatment of different Mn-based alkoxides (5 °C/min, air flow).

Table 2. Full Width at Half Maximum (fwhm) and Related Crystallite Sizes for Mn_3O_4 Samples Prepared by Heating Different Mn-Alkoxides under Air; Data Are Presented for Four Different Bragg Peaks

Bragg peak	fwhm (° 2θ)/crystallite size (Å)				
	Mn-Gly	Mn-Pro12	Mn-EG	Mn-Pro13	Mn-BUT23
(101)	0.96/87	0.95/88	1.01/83	1.51/55	2.9/28
(112)	0.90/95	0.90/95	1.05/81	1.61/53	2.5/34
(103)	0.82/105	1.02/84	1.1/78	1.71/50	2.9/29
(211)	0.91/95	0.88/99	1.1/79	1.80/48	2.7/32
mean crystallite size (Å):	96	91	81	53	31

10 rules out a possible relation between the combustion temperatures and the maxima in BET surface area. Nevertheless, once the organics are burnt, the BET surface areas can still be tuned by a careful selection of the postannealing temperature.

The last aspect of the particles texture that can be controlled is the crystallite size. Figure 11 shows a direct relation between the amount of heat released during the decomposition (ΔH in J/g of oxide) and the Mn_3O_4 crystallite size. The crystallite size of oxides recovered after the combustion was deduced from the full width at half maximum (fwhm) of the XRD Bragg peaks,²⁹ while the total heat was calculated by integrating the

(29) Scherrer, P. *Nachr. Götting Ges.* **1918**, 98.

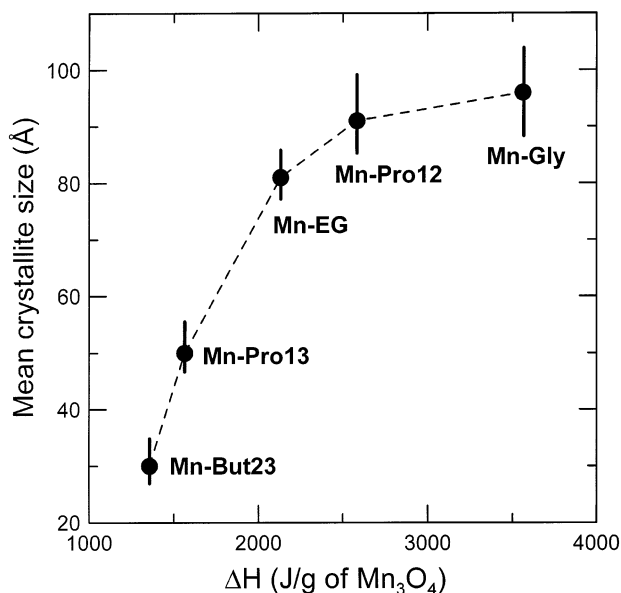


Figure 11. Relation between the mean crystallite size of Mn_3O_4 powders recovered after the combustion of various Mn-based alkoxides and the total amount of heat released during this combustion.

exothermic peaks of the DSC signals as a function of time. Detailed fwhm and crystallite sizes data are displayed in Table 2. Note that the very narrow distribution of these data for various Bragg peaks witnesses the isotropy of the crystallites. This relation between the crystallite size and the heat released during the combustion is in fact not really surprising since the higher the heat provided to the oxide, the easier the sintering/coarsening of the particles/crystallites. A similar trend was observed for Co_3O_4 powders prepared from Co-alkoxides; the oxide crystallite size ranges in this case from 90 to 190 Å.

Once demonstrated that this two-step procedure allows the independent control of (1) the precursors morphology, size, and composition (first step: alkoxides synthesis) and (2) the crystallite size/surface area of the resulting oxides (second step: thermal decomposition), one has to confirm that the initial morphological characteristics of the particles are maintained along the firing treatment. This was verified for all alkoxides and is illustrated in Figure 12, which clearly shows the conservation of the initial morphology and the surface grain growth for Co_3O_4 ex. Co-Pro12. The slight and progressive decrease in the mean sphere size as temperature increases could be ascribed to the particles coarsening and a decrease in porosity that was, for instance, calculated to represent 50% of the apparent volume for the sample treated at 250 °C.

Preliminary tests showed that the thermal decomposition of bimetallic precursors such as (Mn,Co)-Gly or (Mn,Co)-Pro12 led to highly porous mixed oxides at low temperatures. However, this point has not been totally explored and will be the subject of a forthcoming paper.

Conclusions

The results presented in this paper demonstrate that a simple two-step preparation route based on (1) the precipitation of powdered polyol/metal composites and (2) their heat-induced decomposition represent an alternative preparation route for tailored metal oxides particles. That way, various parameters (texture, morphology, and size) of the oxides can be independently controlled by playing with the alcohol composition and the precipitation/decomposition conditions. Several aspects of this method remain to be studied (precipitation temperature, heating duration, solution pH, pyrolysis atmosphere, and counterion) that could enable the control of unexplored parameters such as porosity

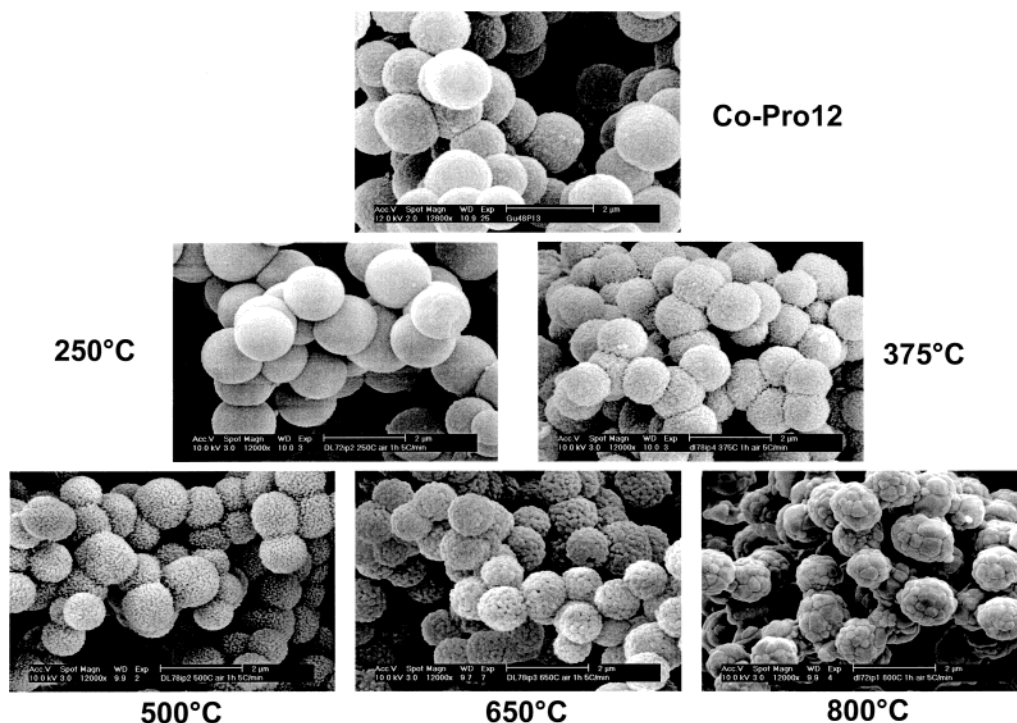


Figure 12. Size and morphology evolution during the Co-Pro12 \rightarrow Co_3O_4 heat-induced reaction and postheating of the resulting Co_3O_4 from 250 to 800 °C (5 °C/min, air flow).

volume and pore size distribution. Apart from the metals presently screened, it is worth keeping in mind that other crystallized polyalcoholates (Fe,⁵ Ni,¹¹ Bi,¹³ Ca,⁷ Al,⁷ Zn,³⁰ Cu, Ti, Cd, Sn, V, Pb, and Sb) can be prepared, witnessing the still unexplored potentialities of this method. There is no doubt that it could be applied to other systems and that as-made tailored powders could be of great value for the accurate study of mechanisms involving interfacial reactions. Finally,

(30) Hambley, T. W.; Snow, M. R. *Aust. J. Chem.* **1983**, *36*, 1249.

preliminary results showed another positive alternative of this method since it can also be used for the preparation of mixed metal oxides.

Acknowledgment. The authors thank Dr. Bernard Gérard (LRCS) and Prof. Ronaldo Herrera-Urbina (University of Sonora, Mexico) for their helpful advice and for sharing their knowledge in the field.

CM030048M